Published in final edited form as:
Plant J. 2014 January ; 77(2): 222–234. doi:10.1111/tpj.12382.

A chemical genetic approach demonstrates that MPK3/MPK6 activation and NADPH oxidase-mediated oxidative burst are two independent signaling events in plant immunity

Juan Xu[1,2,3,#], **Jie Xie**[1], **Chengfei Yan**[4], **Xiaoqin Zou**[4], **Dongtao Ren**[3], and **Shuqun Zhang**[1,2,#]

[1]State Key Laboratory of Plant Physiology and Biochemistry, College of Life Sciences, Zhejiang University, Hangzhou, Zhejiang 310058, China

[2]Division of Biochemistry, Interdisciplinary Plant Group, and Bond Life Sciences Center, University of Missouri, Columbia, Missouri 65211

[3]State Key Laboratory of Plant Physiology and Biochemistry, College of Biological Sciences, China Agricultural University, Beijing 100193, China

[4]Division of Biochemistry, Department of Physics, and Dalton Cardiovascular Research Center, University of Missouri, Columbia, Missouri 65211

Summary

Plant recognition of pathogen-associated molecular patterns (PAMPs) such as bacterial flagellin-derived flg22 triggers rapid activation of mitogen-activated protein kinases (MAPKs) and generation of reactive oxygen species (ROS). Arabidopsis has at least four PAMP/pathogen-responsive MAPKs: MPK3, MPK6, MPK4, and MPK11. It was speculated that these MAPKs may function downstream of ROS in plant immunity because of their activation by exogenously added H_2O_2. MPK3/MPK6 or their orthologs in other plant species were also reported to be involved in ROS burst from the plant respiratory burst oxidase homologue (Rboh) of human neutrophil gp91phox. However, detailed genetic analysis is lacking. Using a chemical genetic approach, we generated another conditional loss-of-function *mpk3 mpk6* double mutant. Together with the conditionally rescued *mpk3 mpk6* double mutant reported previously, we demonstrate that flg22-triggered ROS burst is independent of MPK3/MPK6. In Arabidopsis mutant lacking a functional *AtRbohD*, flg22-induced ROS burst was completely blocked. However, the activation of MPK3/MPK6 was not affected. Based on these results, we conclude that the rapid ROS burst and MPK3/MPK6 activation are two independent early signaling events downstream of FLS2 in plant immunity. We also found that *MPK4* negatively impacts the flg22-induced ROS burst. In addition, salicylic acid-pretreatment enhances AtRbohD-mediated ROS burst, which is again independent of MPK3/MPK6 based on the analysis of *mpk3 mpk6* double mutant. The establishment of a *mpk3 mpk6* double mutant system using the chemical genetic approach offers us a powerful tool to investigate the function of MPK3/MPK6 in plant defense signaling pathway.

[#]Corresponding author: Juan Xu, Tel: 86-571-88982466, Fax: 86-571-88982466, xujuan@zju.edu.cn; Shuqun Zhang, Tel. 573-882-5837, Fax. 573-884-9676, zhangsh@missouri.edu.

Keywords

MAPK cascade; ROS burst; PAMP-triggered immunity; Chemical genetic approach; Salicylic acid

Introduction

Plants have multi-layered defense responses to ward off invading pathogens. The first line of defense is initiated by plant recognition of pathogen-associated molecular patterns (PAMPs), also known as PAMP-triggered immunity (PTI). Several plant receptor-like kinases (RLKs) including FLS2, EFR, and CERK1 have been characterized as PAMP receptors that recognize bacterial flagellin, translational elongation factor-Tu, and fungal cell wall chitin, respectively (Boller and Felix 2009, Gómez-Gómez and Boller 2000, Miya *et al.*, 2007, Wan *et al.*, 2008, Zipfel *et al.*, 2006). Defense responses in PTI are in general transient and are not associated with hypersensitive response (HR) cell death. Bacterial pathogens are capable of secreting effectors into plant cell to facilitate their pathogenesis processes, and plants have evolved to recognize pathogen-derived effectors through resistance proteins. The interaction between the two initiates strong and long-lasting defense responses, known as effector-triggered immunity (ETI), which is frequently associated with HR cell death (Ausubel 2005, Boller and Felix 2009, Chisholm *et al.*, 2006, Dangl and Jones 2001, Jones and Dangl 2006, Martin *et al.*, 2003). In addition to these local responses, the uninfected portions of the plant usually develop systemic acquired resistance (SAR), which is manifested as enhanced resistance to a subsequent challenge by pathogens (Durrant and Dong 2004).

Plant recognition of pathogens triggers several early defense responses including calcium flux, the activation of several mitogen-activated protein kinases (MAPKs), the production of reactive oxygen species (ROS), and the induction of ethylene biosynthesis, which are involved in signaling the intermediate and late defense responses including the activation of a diverse array of defense genes, callose deposition, cell wall strengthening, and phytoalexin biosynthesis (Boller and Felix 2009, Dixon 2001, Glazebrook 2005, Greenberg and Yao 2004, Meng and Zhang, 2013, Torres and Dangl 2005). Genetic analysis in Arabidopsis demonstrated that the early ROS burst is dependent on a NADPH oxidase, AtRbohD, which encodes a respiratory burst oxidase homologue (Rboh) of human neutrophil gp91phox (Torres *et al.*, 2002). In Arabidopsis, PAMPs/pathogens activate two MAPK cascades. MPK3 and MPK6, which share common upstream MAPK kinases (MAPKKs, MEKs, or MKKs), MKK4 and MKK5, form one of the two MAPK cascades. Possible upstream MAPKK kinases (MAPKKKs or MEKKs) include MEKK1 and the ortholog(s) of tomato MAPKKKα (Asai *et al.*, 2002, del Pozo *et al.*, 2004), although it was later disputed whether MEKK1 is the upstream MAPKKK in the MPK3/MPK6 cascade (Ichimura *et al.*, 2006, Nakagami *et al.*, 2006, Suarez-Rodriguez *et al.*, 2007). MPK4, with its upstream MAPKKs, MKK1/MKK2, and MAPKKK, MEKK1 forms the other MAPK cascade (Ichimura *et al.*, 2006, Nakagami *et al.*, 2006, Qiu *et al.*, 2008, Suarez-Rodriguez *et al.*, 2007). Recently, MPK11, a close homolog of MPK4, was shown to be activated in PTI as well (Bethke *et al.* 2012).

MPK3 and MPK6 can also be activated by a number of other stress stimuli including exogenous added H_2O_2 (Kovtun *et al.*, 2000, Yuasa *et al.*, 2001). As a result, it is believed that these MAPKs may function downstream of ROS burst in signaling plant immunity (Apel and Hirt 2004, Kovtun *et al.*, 2000, Pitzschke and Hirt 2009). However, ROS burst is not required for the activation of tobacco SIPK/WIPK and parsley PcMPK6/PcMPK3, the orthologs of Arabidopsis MPK6/MPK3, after treatment with Cf-9 and Pep13, respectively, based on pharmacological analyses (Kroj *et al.*, 2003, Ligterink *et al.*, 1997, Romeis *et al.*, 1999). There are also reports concluding that tobacco SIPK and Ntf4, orthologs of Arabidopsis MPK6, regulate ROS burst from Rboh NADPH oxidase (Asai *et al.*, 2008, Yoshioka *et al.*, 2003). This conclusion was challenged by two recent reports that concluded MPK3/MPK6 and their homologs in tobacco are not required for the elicitor-triggered ROS burst (Galletti *et al.*, 2011, Segonzac *et al.*, 2011). However, detailed genetic analyses using stable transgenic and mutant plants are still lacking. Functional redundancy and embryo lethality of the *mpk3 mpk6* double mutant make it difficult to clarify their roles in specific signaling pathways. Using a conditional rescue strategy (Wang *et al.*, 2007) and a chemical genetic approach (in this report), we generated two systems in which MPK3 and MPK6 signaling can be specifically blocked. They allowed us to clarify the relationship between MAPK activation and ROS burst, two early signaling events after plant sensing of invading pathogens. In both systems, we found that flg22, a peptide PAMP derived from bacterial flagellin, triggered normal ROS burst. In Arabidopsis *atrbohD* mutant, flg22-induced ROS burst was completely blocked. However, the activation of MPK3 and MPK6 was not affected. In contrast, both MAPK activation and ROS burst were completely abolished in *fls2* mutant. Based on these results, we conclude that oxidative burst and MAPK activation are two independent signaling events downstream of FLS2 in plant immunity and demonstrate that the chemical genetic approach can be a powerful tool in analyzing the functions of gene(s) essential for embryogenesis.

Results

Activation of MPK3/MPK6 is not sufficient to induce the early ROS burst and fail to enhance flg22-triggered ROS burst

HR-like cell death induced by the activation of Arabidopsis MPK3/MPK6 or tobacco SIPK/WIPK/Ntf4 in the DEX-inducible promoter-driven *NtMEK2*^{DD} (*GVG: NtMEK2*^{DD}, abbreviated as *DD*) transgenic plants is associated with ROS generation (Ren *et al.*, 2002). Further analyses revealed that the ROS in the *DD* plants originate in chloroplasts as a possible result of metabolic imbalance (Liu *et al.*, 2007). Similar to *DD* tobacco plants, DEX treatment of *DD* Arabidopsis plants also triggered ROS generation in chloroplasts as detected by DAB staining (Figure 1a). However, luminol-based method failed to detect any ROS generation originated from NADPH oxidases (Figure 1b). There was no difference between *DD* and the negative control plants that carry an inactive mutant of *NtMEK2* with the catalytic essential Lys (K) mutated to Arg (R) (*GVG-NtMEK2*^{KR}, abbreviated as *KR*) (Ren *et al.*, 2002). Activation of MPK3/MPK6 was detectable as early as 1 hr after DEX treatment, and reached maximum at 3 hr after DEX treatment (Figure 1c). As a result, we conclude that MPK3/MPK6 activation is not sufficient to induce the Rboh-based cell surface

ROS burst, which is different from previous reports using the *Agrobacterium*-mediated transient overexpression tobacco system (Asai *et al.*, 2008, Yoshioka *et al.*, 2003).

We then determined whether MPK3/MPK6 activation is able to enhance the ROS burst triggered by flg22, a bacterial flagellin-derived PAMP. In this experiment, we treated *DD* seedlings with DEX for 3 hr, and then with flg22. As shown in Figure 1d, pre-activation of MPK3/MPK6 did not enhance the ROS burst triggered by flg22 treatment. To its contrary, ROS burst was reduced in *DD* seedlings pretreated with DEX, which activated MPK3/MPK6 (Figure 1c) (Ren *et al.*, 2002). In the *KR* control transgenic seedlings without MPK3/MPK6 activation (Figure 1c) (Ren *et al.*, 2002), ROS generation was higher than that in the *DD* seedlings after flg22 treatment (Figure 1d). To exclude a potential dominant negative effect of the *KR* transgene, we also compared the *KR* with empty vector (*EV*) control seedlings after flg22 treatment. There was no significant difference in ROS generation between the two (Figure 1d). After DEX-pretreatment for 3 hours, flg22 treatment of *KR* and *EV* seedlings showed similar MAPK activation patterns (Figure S1). *DD* seedlings pretreated with DEX for 3 hours had high MPK3/MPK6 activities, and flg22 treatment showed little enhancement. In contrast, MPK4 could still be activated by flg22 in *DD* seedlings pretreated with DEX (Figure S1) despite at a lower level.

To support the observation that MPK3/MPK6 activation might negatively impact the ROS burst induced by flg22, we also examined the ROS burst in transgenic *35S:MPK6* seedlings that overexpress *MPK6* (*MPK6* OE) after flg22 treatment. As shown in Figure S2a, *35S:MPK6* seedlings produced less ROS than the empty vector control transgenic seedlings. Immunoblot analysis confirmed the overexpression of MPK6 (Figure S2b), and in-gel kinase assay demonstrated the hyperactivation of MPK6 as a result of combined activation of endogenous MPK6 and Flag-epitope tagged MPK6 (F-MPK6) after flg22 treatment (Figure S2c). There are two potential explanations for such observation. Firstly, it is possible that MPK3/MPK6 activation partially inhibits ROS burst directly. Alternatively, it is possible that the reduction is a result of cellular metabolic changes after the activation of MPK3/MPK6, i.e. the reduction in ROS burst is an indirect effect of MPK3/MPK6 activation.

MPK3/MPK6 activation is not required for the *AtRbohD*-originated ROS burst

Exogenously applied H_2O_2 rapidly activates plant MAPKs including Arabidopsis MPK3 and MPK6, which led to the speculation that MAPK may function downstream of ROS in the plant stress/defense signaling (Apel and Hirt 2004, Kovtun *et al.*, 2000, Yuasa *et al.*, 2001). We also observed rapid activation of MAPKs in Arabidopsis seedlings treated with H_2O_2 (Figure S3). Based on the analysis of *mpk3*, *mpk6*, and *mpk4* mutants, H_2O_2 activated MPK3, MPK6, and MPK4. The kinase activity corresponding to the size of MPK4 was not completely abolished in the *mpk4* mutant, suggesting that this kinase band involves additional kinases, possibly homologs of MPK4 in the Group B of plant MAPKs such as MPK11 (Bethke *et al.*, 2012, Ichimura *et al.*, 2002). To determine whether the rapid ROS burst is required for the activation of MAPKs in response to flg22, we examined the MAPK activation in *atrbohD* mutant. As previously reported (Mersmann *et al.*, 2010, Ranf *et al.*, 2011, Zhang *et al.*, 2007), no ROS burst was detected in *atrbohD* seedlings after flg22

treatment (Figure S4a). However, MAPK activation was normal (Figure S4b), demonstrating that the ROS burst is not required for the MAPK activation triggered by flg22. Rapid activation of MAPKs and ROS burst after flg22 treatment are both dependent on FLS2. In *fls2* mutant, both events were inhibited (Figure S4c and S4d), which suggests that ROS burst is not required for the MAPK activation in Arabidopsis after FLS2-mediated sensing of flg22.

To obtain loss-of-function data to determine the role of MPK3 and MPK6 in flg22-induced ROS burst, we compared the ROS production in *mpk3* and *mpk6* single mutant and the wild-type control seedlings. As shown in Figure 2a, ROS generation in *mpk3* and *mpk6* single mutant seedlings was identical to that in Col-0 wild type in both the magnitude and kinetics, possibly a result of the functional redundancy between *MPK3* and *MPK6*. *MPK3* and *MPK6* play an essential role in embryogenesis, and double *mpk3 mpk6* mutant zygotes are embryo lethal. We previously generated a conditionally rescued double *mpk3 mpk6* mutant by transforming a DEX-inducible promoter-driven *MPK6* (*GVG:MPK6*) into *mpk3 mpk6*$^{+/-}$ plants (Wang *et al.*, 2007). During the flowering stage of the T3 *mpk3 mpk6*$^{+/-}$ *GVG:MPK6* plants, spraying of DEX allowed us to rescue the embryo lethality of the double mutant zygotes. Progenies with *mpk3 mpk6 GVG:MPK6* genotype were called rescued *mpk3 mpk6* double mutant, and were used for experiments. As shown in Figure 2b, the rescued *mpk3 mpk6* double mutant seedlings showed similar levels of ROS burst as the wild type, demonstrating that *MPK3/MPK6* are not essential for the ROS burst. The slightly different kinetics of ROS production in the *mpk3 mpk6* seedlings after flg22 treatment might be a result of the developmental defects of the seedlings (Wang *et al.* 2007).

As previously reported, flg22 treatment activated both MPK3 and MPK6 (Figure 2c, top panel). In their respective mutants, either MPK3 or MPK6 activity was absent. In the rescued *mpk3 mpk6* double mutant, both MPK3 and MPK6 activities were abolished. However, the activity of MPK4 was much higher, a phenomenon also observed in the rescued *mpk3 mpk6* double mutant after the inoculation of *Botrytis cinerea* spores (Ren *et al.*, 2008). In the rescued *mpk3 mpk6* double mutant seedlings, MPK4 protein level was higher (Figure 2c, middle panel), which may partially contribute to the higher MPK4 activation after flg22 treatment.

A *mpk3 mpk6* double mutant system based on a chemical genetic approach also demonstrates that MPK3/MPK6 are not involved in the AtRbohD-mediated ROS burst

Conditional rescue of *mpk3 mpk6* double mutant using *GVG:MPK6* construct allowed the discovery of additional functions of these two MAPKs in plant development and loss-of-function analysis of these two MAPKs in plant defense/stress response (Han *et al.*, 2010, Ren *et al.*, 2008, Wang *et al.*, 2007) (this report). However, *mpk3 mpk6 GVG:MPK6* plants are developmentally arrested at seedling stage even in the presence of DEX. We found that only the native promoter-driven *MPK6* or *MPK3* can fully rescue the double mutant, suggesting the importance of spatiotemporal expression patterns of these two MAPKs. In order to acquire loss-of-function data from a developmentally normal *mpk3 mpk6* plants, we used the chemical genetic approach developed in Shokat lab (Bishop *et al.*, 2000), and generated another *mpk3 mpk6* double mutant system.

Sequence/structure based analyses identified the Tyr144 (Y144) as the potential gate-keeping amino acid in the ATP-binding pocket of MPK6 (Figure 3). Kinase inhibitor PP1 (4-amino-1-tert-butyl-3-(4-methylphenyl)pyrazolo[3,4-d]pyrimidine) can access the ATP-binding pocket of a wild-type kinases and inhibit them. However, NA-PP1 (4-amino-1-tert-butyl-3-(1′-naphthyl)pyrazolo[3,4-d]pyrimidine), a PP1 analog with a bulkier side chain, cannot enter the ATP-binding pocket of a wild-type kinase because of atom clash with the gate-keeping amino acids such as the Y144 in MPK6. When the large Y144 amino acid in MPK6 is mutated to a smaller amino acid such as Gly (G), NA-PP1 should be able to access the ATP-binding site of the kinases and inhibit their activity (Figure 3, right panel). This way, NA-PP1 can be used potentially as a specific inhibitor of the sensitized MPK6^{YG} kinase in the transgenic plants. In the absence of NA-PP1, MPK6^{YG} protein can be functional, allowing it to rescue the embryo lethality of *mpk3 mpk6* double mutant.

Following this experimental design, native promoter-driven *MPK6*^{YG} (*P*$_{MPK6}$*:MPK6*^{YG}) was transformed into *mpk6* mutant plants. *MPK6*^{YG} *mpk6* transgenic plants were then crossed with pollen from *mpk3*$^{+/-}$ *mpk6* plants. In the absence of NA-PP1, MPK6^{YG} is functional, therefore, allowed the rescue of the embryo lethality of *mpk3 mpk6* double mutant and the generation of normally developed MPK6^{YG}-rescued plants, which are named inhibitor-sensitized MPK6 variant-rescued *mpk3 mpk6* double mutant plants, or*MPK6SR* for short (genotype *mpk3 mpk6 P*$_{MPK6}$*:MPK6*^{YG}). Multiple lines were obtained and one line (*MPK6SR31*) was shown (Figure 4a). The level of MPK6^{YG} expression was similar to that of the endogenous MPK6 based on the immunoblot analysis using an anti-MPK6 antibody (Figure 4c).

To determine whether MPK6^{YG}, the potentially sensitized form of MPK6, is indeed sensitive to NA-PP1, we used the in-gel kinase activity assay to compare the activity of MPK6^{YG} and MPK6 in the absence and presence of NA-PP1. To activate MAPKs, we treated two-week-old wild-type (Col-0) and *MPK6SR* seedlings with flg22 for 10 and 30 min. Protein extracts, which contain the activated MAPKs, were prepared for in-gel kinase assay. In wild-type seedlings, flg22 activated three MAPKs, MPK6, MPK3, and MPK4 (Figure 4b, upper panel)(Liu and Zhang 2004, Suarez-Rodriguez *et al.*, 2007). In *MPK6SR* seedlings treated with flg22, the activity at the position of MPK6 was from MPK6^{YG} variant, and no MPK3 activity was present (Figure 4b, upper panel). When the in-gel kinase assay was performed in the presence of 0.02 μM NA-PP1 in the reaction solution (Figure 4b, lower panel), the activities of MPK6, MPK3, and MPK4 from the wild-type seedlings and MPK4 from the *MPK6SR* seedlings were not affected. In contrast, the activity of MPK6^{YG} from the *MPK6SR* seedlings was completely inhibited, revealing that MPK6^{YG} is highly sensitive to NA-PP1 while the wild-type endogenous MAPKs are not inhibited by NA-PP1.

Due to the non-covalent nature of NA-PP1 inhibition of MPK6^{YG}, it is not possible to demonstrate the *in vivo* effectiveness of NA-PP1 inhibitor using *in vitro* biochemical assays such as in-gel kinase assay. As a result, we used stomatal phenotype of the *mpk3 mpk6* double mutant as an indicator of NA-PP1 effectiveness *in vivo*. Based on genetic analyses, stomatal development has the lowest requirement of MPK3/MPK6 activity. In plants that showed abscission, ovule development, or flower clustering phenotype (Cho *et al.*, 2008, Meng *et al.*, 2012, Wang *et al.*, 2008), stomatal patterning is normal. Stomatal clustering

phenotype is only observed in *mpk3 mpk6* double mutant (Wang *et al*., 2007). As a result, stomatal phenotype is the best indicator of NA-PP1 effectiveness *in vivo*. We tested different concentrations of NA-PP1 (0.1-10 μM) to determine the effective concentration. *MPK6SR* seedlings could recapitulate the clustered stomata phenotype of *mpk3 mpk6* double mutant in the presence of as low as 0.5 μM NA-PP1 (Figure 4d, lower right panel) (Wang *et al*., 2007). In contrast, *MPK6SR* seedlings grown on plates with DMSO solvent and Col-0 seedlings grown on plates with NA-PP1 or DMSO developed normal epidermal layer (Figure 4d). In a hydroponic culture system, *MPK6SR* plants treated with 1 μM NA-PP1 inhibitor also had clustered flower (Figure S5), which is similar to the loss-of-function mutants of *YDA* and *ER/ERL1/ERL2* (Lukowitz *et al*., 2004; Shpak *et al*., 2004), two upstream signaling components of MPK3/MPK6 (Meng *et al*., 2012). These results demonstrate that NA-PP1 is effective *in vivo* in inhibiting the activity of $MPK6^{YG}$, but not the wide-type MPK6, and *MPK6SR* plants could allow us to achieve activity null mutant of MPK3 and MPK6 by applying NA-PP1 inhibitor.

Using this system, we demonstrated again that MPK3 and MPK6 are not essential to the flg22-induced ROS burst. After we found out the minimal NA-PP1 concentration (0.5 μM) to induce a full stomatal phenotype (epidermal layer of the newly developed leaves only had guard cells), an indication of complete inhibition of $MPK6^{YG}$ activity, we used 1 μM NA-PP1 for all the ROS burst experiments. As shown in Figure 4e, there was little difference in the ROS burst in the absence or presence of NA-PP1 inhibitor. We also tried different lengths of NA-PP1 pretreatment, and similar results were obtained (Figure S6). Figure 4e shows the results with 30 min NA-PP1 pretreatment. Based on the analysis of two different loss-of-functional *mpk3 mpk6* double mutant systems, we conclude that MPK3/MPK6 are not required for the *AtRbohD*-mediated ROS burst in Arabidopsis after flg22 treatment. Together with other data, we can conclude that ROS burst and MPK3/MPK6 activation are two independent early signaling events in Arabidopsis after FLS2-mediated sensing of flg22.

MPK3 and MPK6 are not essential for the salicylic acid (SA)-induced potentiation of ROS production in response to flg22 treatment

As a signaling molecule in systemic acquired resistance, SA-pretreatment can potentiate a number of plant defenses. Cultured soybean cells pre-treated with SA produced much higher levels of ROS after pathogen treatment (Shirasu *et al.*, 1997). To determine whether SA can enhance the ROS production induced by flg22, we pre-treated Arabidopsis seedlings with 100 μM SA for 2 days before measuring flg22-induced ROS burst. As shown in Figure 5a, wild-type seedlings with SA-pretreatment produced much higher levels of ROS after flg22 treatment. In addition, the ROS production peaked earlier, suggesting that Arabidopsis seedlings pretreated with SA were potentiated to produce ROS after the sensing of PAMP molecule. The higher level of ROS production in SA-pretreated Arabidopsis was completely dependent on *AtRbohD* (Figure 5a).

Similar to other SA-potentiated defense responses, the enhanced ROS production is also dependent on *NPR1*. In *npr1* mutant, the enhanced ROS production in SA-pretreated seedlings was abolished (Figure 5b). In addition, the presence of *NahG* transgene, which

encodes a bacterial salicylate hydroxylase enzyme that converts SA to catechol, also abolished the enhanced ROS burst (Figure 5c). Furthermore, we consistently observed slightly lower ROS burst in *NahG* plants, suggesting that basal SA level might be involved in the ROS burst as well (Figure 5c).

To determine whether the enhanced ROS production after SA pretreatment is associated with higher level of *AtRbohD* gene expression after SA treatment, we used real-time RT-PCR to compare the expression of *AtRbohD* in samples with and without SA pretreatment. As shown in Figure S7 (0 min time point) SA-pretreatment did not elevate the expression of *AtRbohD* gene. In addition, the induction of *AtRbohD* in SA-pretreated seedlings after flg22 treatment was similar to that in the seedlings without SA pretreatment, with the exception of late time point. The higher gene activation at 60 min after flg22 treatment was dependent on *NPR1* and was abolished by the *NahG* transgene (Figure S7). The flg22-induced *AtRbohD* expression is unlikely to contribute to the rapid ROS burst because of delayed induction kinetics of *AtRbohD* transcript. Among all the *Rboh* genes in Arabidopsis seedlings *AtRbohD* has the highest basal level expression (Figure S8). All of these suggest that the post-translational regulation of AtRbohD activity instead of the transcriptional activation of *AtRbohD* gene plays an important role in the rapid ROS burst.

MPK3/MPK6 was not essential for flg22-induced ROS burst (Figure 2 and 4). To determine whether this MAPK cascade is involved in the SA-potentiation of ROS burst induced by flg22, we pre-treated *MPK6SR* seedlings with SA or DMSO for 2 days. The seedlings were then pre-treated with NA-PP1 inhibitor (1 μM) for 30 min before the addition of flg22, and ROS production was monitored by photon-counting camera after the addition of flg22. As shown in Figure 6, pre-treatment with NA-PP1 did not interfere with the SA-induced potentiation of ROS burst, suggesting that MPK3/MPK6 cascade is not involved in the enhanced ROS burst in SA-pretreated seedlings either.

Mutation of *MPK4* enhances the flg22-induced ROS burst

Besides MPK3 and MPK6, flg22 also activates MPK4. Similar to *mekk1* mutant, soil-grown *mpk4* mutant plants accumulate higher levels of H_2O_2 in their leaves (Nakagami *et al.*, 2006). However, the source(s) of H_2O_2 production in *mpk4* mutant was not determined in the study. Tobacco *Ntf6*, a potential ortholog of Arabidopsis *MPK4* was reported as a positive regulator of Rboh-mediated ROS burst (Asai *et al.*, 2008). Therefore, we also examined the ROS production in *mpk4* mutant. We used 14-day-old *mpk4* mutant seedlings, which do not have the developmental defects yet (Mao *et al.*, 2011). As shown in Figure 7a (0 min), basal level ROS production in *mpk4* mutant seedlings was similar to that in the wild type (Ler-0). Interestingly, with flg22 treatment, *mpk4* mutant seedlings produced much higher levels of ROS, and the ROS induction peaked earlier than in the wild-type seedlings (Figure 7a). The enhancement of ROS burst in *mpk4* mutant is similar to that after SA treatment (Figure 5a), which is consistent with the conclusion that MPK4 negatively regulates the SAR response (Petersen *et al.*, 2000). In supporting of this, we found that two-weeks old *mpk4* seedlings, despite of the lack of obvious developmental phenotype, did have elevated levels of *PR1* gene expression (Figure S9), an indication of the activation of SAR pathway. In *mpk4* mutant, flg22 treatment failed to activate the smallest kinase band in

comparison to the activation of all three kinase bands (MPK6, MPK3, and MPK4 in decreasing size) in the Ler-0 wild-type control (Figure 7b). Immunoblot analysis using the anti-MPK4 antibody demonstrated the lack of MPK4 protein in the *mpk4* mutant seedlings (Figure 7c). This experiment also showed that the antibody is specific for MPK4, and does not recognize its close homologs in the Group B of plant MAPKs including MPK11 (Ichimura *et al.*, 2002).

Discussion

MAPK activation and ROS burst are two early events in PAMP-triggered immunity. Flg22, a well-characterized bacterial PAMP derived from bacterial flagellin, rapidly activates MPK3, MPK6, and MPK4 in Arabidopsis plants/seedlings. Using a conditional rescuing strategy and a chemical genetic approach, we generated two systems in which MPK3 and MPK6 signaling can be blocked. In both loss-of-function systems, we found that flg22 triggers normal ROS burst. The activation of MPK3 and MPK6 was not affected in the *AtRbohD* mutant, suggesting that the rapid activation of MAPKs in Arabidopsis after flg22 treatment is not a result of the H_2O_2 burst despite strong activation of these MAPKs by exogenous H_2O_2 treatment. In contrast, both MAPK activation and ROS burst were completely abolished in mutant lacking a functional FLS2. We also found that SA potentiates flg22-induced ROS burst, which is MPK3/MPK6 independent, but *AtRbohD* and *NPR1* dependent. In *mpk4* mutant, flg22 induces a heightened ROS burst. Figure 8 is our current working model summarizing the relationships between ROS burst and MAPK activation, two early signaling events downstream of plant sensing of PAMPs/pathogens.

MPK3/MPK6 activation and Rboh-mediated ROS burst are two independent early events in plant immunity

It was reported that the expression of constitutively active StMEK2 and NbMEK1, which are orthologous to tobacco NtMEK2 and NtMEK1, respectively, induces the Rboh-dependent ROS generation in a tobacco transient expression system (Asai *et al.*, 2008, Yoshioka *et al.*, 2003). In this report, we demonstrate that the activation of MPK3/MPK6 in *DD* plants is not sufficient to trigger *Rboh*-mediated ROS burst (Figure 1b). To the contrary, MPK3/MPK6 activation in *DD* plants was associated with a reduced ROS burst after flg22 treatment (Figure 1d). The discrepancy is unlikely to be a result of different plant species. As we reported earlier, activation of SIPK, WIPK, and Ntf4 failed to trigger Rboh-mediated ROS burst in *DD* transgenic tobacco plants as well (Liu *et al.*, 2007). Instead, The ROS accumulation in *DD* plants before HR-like cell death originates in the chloroplasts (Figure 1a) (Liu *et al.*, 2007, Ren *et al.*, 2002).

It is also quite unusual that the overexpression of SIPK or Ntf4 using *Agrobacterium*-infiltration method is sufficient to trigger ROS burst (Asai *et al.*, 2008). We failed to observe ROS burst in plants overexpressing MPK6, the Arabidopsis ortholog of tobacco SIPK (Figure S2). In general, overexpression of MAPKs is not sufficient to cause the increase in MAPK activity without the presence of a suitable stimulus, and therefore, no downstream response will be triggered. In our experimental conditions, overexpression of MPK6 is not associated with an increase in MPK6 activity (Figure S2c, 0 min time point), consistent with

the general concept that MAPKs need phosphorylation activation by their upstream MAPKKs. In Asai et al. (2008) report, the activity of MAPKs in the transiently transformed tobacco leaves was not examined.

ROS accumulation in the *DD* tobacco plants before HR-like cell death is localized in chloroplasts (Liu *et al.*, 2007). Chloroplast-originated ROS were also detectable in *DD* Arabidopsis after DEX treatment (Figure 1a). In the discussion of Asia et al. 2008 paper, our conclusion in Liu et al., 2007 paper was misstated. We concluded that the activation of SIPK/WIPK does not result in the earlier ROS burst, but is involved in the ROS generation at the late stage before HR-like cell death. We did not make any conclusion as stated in Asai et al. 2008 paper, Page 1397: “They concluded that the chloroplast burst occurs earlier than the NADPH oxidase-dependent oxidative burst by MAPK (phase II burst) and that the chloroplast-generated ROS are only a facilitator that accelerates cell death because plants cells without mature chloroplasts die eventually.” It is known that the rapid ROS burst (Phase I) is Rboh-related, while the later stage ROS generation (Phase II) may have many sources including organelles such chloroplasts and mitochondria in plant defense response (Apel and Hirt 2004, Lamb and Dixon 1997). Chloroplast-localized ROS are detectable only after many hours of MPK3/MPK6 or SIPK/WIPK activation (Figure 1a) (Liu *et al.*, 2007), possibly a result of metabolic imbalance in the chloroplasts. If MPK3/MPK6 or their orthologs in other plant species were involved in PAMP- or pathogen-triggered Rboh-dependent ROS burst, one would expect a very rapid induction of ROS production after MAPK activation.

Our observation that MPK3/MPK6 may negatively impact the flg22-induced ROS burst (Figure 1 and S2) is consistent with recent findings that mutation of *MPK3* or silencing of *SIPK* and/or *WIPK* lead to prolonged or/and enhanced ROS burst in response to flg22 (Ranf *et al.*, 2011, Segonzac *et al.*, 2011). Under our experimental conditions, only *mpk3 mpk6* double mutant showed slightly prolonged ROS accumulation (Figure 2b and 4e) and no enhanced or prolonged ROS burst in either single mutant (Figure 2a). The variation might result from different systems and experimental conditions. In Segonzac et al (2011) paper, the presence of *Agrobacteria* in the transient transformation or virus in the VIGS system could have an impact on the response of plants. The much higher concentration of flg22 (1 μM versus 30 nM in our study) and leaf discs from soil-grown plants in Ranf et al (2011) report could also cause the difference. Based on our evidence from conditional *mpk3 mpk6* double mutant systems, together with several lines of evidence obtained by other groups (Galletti *et al.*, 2011, Ranf *et al.*, 2011, Segonzac *et al.*, 2011), we can conclude now that the MPK3/MPK6 activation and ROS burst in response to flg22 are two independent signaling events. However, the MPK3/MPK6 activation can influence, likely indirectly, ROS accumulation in response to PAMPs at the late stage.

Enhanced ROS burst in SA-pretreated seedlings is not dependent on MPK3/MPK6

As an important signaling molecular in plant SAR, SA treatment enhances a number of defense-related responses (Durrant and Dong 2004). MPK4 is a negative regulator of plant defense, and its mutation causes constitutive accumulation of SA and SAR in the *mpk4* mutant (Petersen *et al.*, 2000). As a result, we examined the flg22-induced ROS burst in

mpk4 mutant and the role of SA in AtRbohD-mediated ROS burst. We found that pretreatment of seedlings with SA potentiates the flg22-triggered H_2O_2 burst (Figure 5) and mutation of *MPK4* enhances the flg22-induced ROS burst (Figure 7) which might be a result of higher SA levels in the *mpk4* seedlings. Consistent with this speculation, *mpk4* seedlings have elevated *PR1* gene expression despite of the lack of the developmental phenotype of the soil-grown plants (Figure S9)(Mao *et al.*, 2011; Petersen *et al.*, 2000). Similar to other SA-induced defense responses, the enhancement of H_2O_2 production is dependent on functional *NPR1* and was abolished in *NahG* plants. In *atrbohD* mutant, both normal and SA-enhanced H_2O_2 production are inhibited, suggesting the enhancement is through the action on *AtRbohD* gene and/or protein. Real-time qPCR revealed a slight enhancement of *AtRbohD* gene activation at later stage (60 min) after flg22 treatment in SA-pretreated seedlings (Figure S8). However, it is too late to account for the rapid H_2O_2 burst. Previously, it was shown that SA pretreatment could enhance H_2O_2 accumulation in soybean suspension cultured cells (Shirasu *et al.*, 1997). Here, we provide genetic evidence the potentiation is also dependent on *NPR1*, an important component in SA signaling pathway. Since SA can activate SIPK in tobacco (Zhang and Klessig 1997), we examined whether MPK6, the Arabidopsis ortholog of SIPK, and MPK3 are involved in the potentiation of flg22-triggered ROS burst. As shown in Figure 6, blockage of both MPK3 and MPK6 does not affect the enhanced ROS burst in SA-pretreated Arabidopsis.

Chemical genetic approach as a powerful tool to investigate MPK3/MPK6 functions

MPK3 and MPK6 play redundant functions in multiple biological processes (Rodriguez *et al.*, 2010, Zhang 2013). They are also essential for the first asymmetric cell division of zygotes, and the loss of both MAPKs resulted in embryo lethal phenotype (Wang *et al.*, 2007), which makes it very difficult to gain loss-of-function evidence. In this study, we used a chemical genetic approach first developed by Shokat group (Bishop *et al.*, 2000) and generated a WT-like *mpk3 mpk6* double mutant plants/seedlings (genotype *mpk3 mpk6* P_{MPK6}:$MPK6^{YG}$), in which the activity of $MPK6^{YG}$ can be inhibited by the application of NA-PP1 inhibitor at any stage (Figure 3, 4 and S5). This strategy provides a powerful tool for us to determine the functions MPK3 and MPK6 in plant defense without the complications from the developmental defects associated with the loss of both *MPK3* and *MPK6*.

RNAi gene silencing or overexpression of MAPK activity suppressor including Ser/Thr phosphatase AP2C1 or the *Pseudomonas syringae* effector HopAI1 have been used to knock down the expression of *MPK3* and *MPK6* genes or inhibit the activation of MPK3 and MPK6 (Galletti *et al.*, 2011, Schweighofer *et al.*, 2007, Segonzac *et al.*, 2011, Wang *et al.*, 2007, Zhang *et al.*, 2007). In these systems, the suppression of MPK3 and MPK6 is not complete. Otherwise, the embryogenesis will be affected and no viable seeds could be obtained. In addition, off-target gene silencing may be present, and phosphatase and effector proteins most likely have multiple targets. The chemical genetic strategy used in this study provides a stable system to facilitate the loss-of-function studies of MPK3 and MPK6. The possibility of co-silencing or off-target silencing of other homologs by RNAi or inactive other substrates by phosphatase or effector can be avoided.

In summary, we demonstrate that the activation MPK3/MPK6 cascade is an event independent of AtRbohD-mediated ROS burst in flg22-triggered plant immunity, as depicted in Figure 8. In this study, we also generated a *mpk3 mpk6* double mutant using a chemical genetic approach. This *mpk3 mpk6* double mutant system provides a powerful tool for us to further study the functions of MPK3 and MPK6. This chemical genetic approach can also be used for function analyses of other kinases that are multi-functional and essential to embryogenesis.

Experimental Procedures

Plant growth and treatments

Arabidopsis thaliana wild-type plants, mutants and transgenics were all in the Col-0 ecotype background with the exception of *mpk4-1*, which is in Ler-0 ecotype. Soil-grown plants were maintained at 22 °C in a growth chamber with a 14-hr light cycle (100 μE m^{-2} sec^{-1}). For experiments, seedlings were grown in half-strength MS medium at 22 °C under continuous light (70 μE m^{-2} sec^{-1}). Unless indicated otherwise, two-week-old seedlings were used for the experiments. Dexamethasone (DEX) and flg22 PAMP were used at final concentrations of 1 μM and 30 nM, respectively. SA and NA-PP1 stock solutions were prepared in DMSO, and used at indicated final concentrations. Equal volume of DMSO was used as negative controls. In the luminol-based ROS assay, NA-PP1 treatment was performed by the addition of NA-PP1 stock solution to the bathing medium. For the stomatal induction assay, *MPK6SR* or wild-type control seedlings were transferred to MS plates with different concentrations (0.1 – 10 μM) of NA-PP1 inhibitor, which were prepared similarly as other selection plates.

For observation of the effect of NA-PP1 inhibitor on the stomatal development of *MPK6SR* seedlings, the seeds were first germinated on the MS plates without NA-PP1. Five-days later, the seedlings were moved onto plates with NA-PP1 inhibitor (0.5 μM) or DMSO solvent control, and the newly emerged true leaves were sampled for microscopic observation and imaging. To determine the effect of NA-PP1 on the inflorescence development, we first grew the *MPK6SR* plants hydroponically as described (Tocquin *et al*. 2003). NA-PP1 inhibitor (1 μM) was added into the medium just before the plants started to bolt. The pictures were taken a week later.

At least two independent repetitions were performed for experiments with multiple time points. For single time-point experiments, at least three independent repetitions were done. Statistical analysis was performed using GraphPad InStat 6.0 (http://www.graphpad.com/). Single and double asterisks above the data points indicate differences that are statistically significant (Student's *t*-test, $p<0.05$) and statistically very significant (Student's *t*-test, $p<0.01$), respectively. When more than two groups of samples are compared, Kruskal–Wallis/Dunn's post-test was used. Different letters (a, ab, and b) above the data points are used to indicate differences that are statistically significant ($P < 0.05$).

Mutants and transgenic lines

T-DNA insertional *mpk3* (Salk_151594) and *mpk6* (Salk_073907 and Salk_127507) mutants were obtained from the Arabidopsis Biological Resource Center (Alonso *et al.*, 2003, Liu and Zhang 2004, Wang *et al.*, 2007). Transposon-induced *mpk4* mutant in Ler-0 background was kindly supplied by Dr. John Mundy (Petersen *et al.*, 2000). Transgenic *NahG* and *npr1* mutant seeds were kindly supplied by Dr. Xinnian Dong. The steroid-inducible *GVG:NtMEK2*^{DD} transgenic line and the conditionally *GVG:MPK6* rescued *mpk3 mpk6* double mutant were described in Ren et al. (2002) and Wang et al. (2007), respectively.

Identification of gate-keeping amino acid in the ATP-binding pocket of MPK6

The three-dimensional atomic model of MPK6 was constructed based on the crystal structure of human ERK2 (i.e., MAPK1; PDB entry: 1WZY) (Kinoshita *et al.*, 2006) using the MODELLER software (Marti-Renom *et al.*, 2000). The structure of MPK6^{YG} was modeled by mutating Y144 of MPK6 to glycine with the Chimera software (Pettersen *et al.*, 2004). The three-dimensional atomic structure of NA-PP1 was built using Chimera, based on the crystal structure of PP1 taken from the ligand in the PDB entry, 2IVV (Knowles *et al.*, 2006). The binding mode of PP1 to MPK6 and NA-PP1 to MPK6^{YG} was produced by superimposing MPK6 to the crystal structure of RET tyrosine kinase bound with PP1 (PDB entry: 2IVV) using Chimera.

Generation of the conditional *mpk3 mpk6* double mutant using a chemical genetic approach

To generate NA-PP1 inhibitor-sensitive MPK6 variant, we mutated Tyr144 residue in the ATP-binding pocket of MPK6 to Gly (MPK6^{YG}). A *MPK6* native promoter-driven *MPK6* cDNA in pCambia3300 vector with this mutation (P_{MPK6}:*MPK6*^{YG}) was transformed into *mpk6* plants. Four independent single-insertion lines with *MPK6*^{YG} expressed at a similar level as the endogenous *MPK6* gene were identified by immunoblot analysis using an anti-MPK6 antibody (Sigma, St. Louis). They were then crossed with *mpk3*$^{+/-}$ *mpk6* plants (pollen donor) to generate *mpk3*$^{+/-}$ *mpk6* P_{MPK6}:*MPK6*$^{YG+/-}$ plants. F3 homozygous P_{MPK6}:*MPK6*^{YG} transgenic plants in *mpk3 mpk6* background (*mpk3 mpk6* P_{MPK6}:*MPK6*^{YG}), also called inhibitor-sensitized MPK6 variant-rescued plants (*MPK6SR*) were used for experiments. Two independent transgenic lines were followed and the same results were obtained.

Detection of ROS generation by DAB staining and luminol-based assays

In vivo H_2O_2 generation in plants was detected by an *in situ* histochemical staining procedure using 3,3′-diaminobenzidine (DAB) (Thordal-Christensen *et al.*, 1997). The procedure was performed as described in Ren et al. (2002).

Luminol-based luminescence method was used to detect the ROS burst (Gómez-Gómez *et al.*, 1999). Briefly, true leaves were detached from 2-week-old seedlings and transferred to 24-or 48-well plates with 1 mL of water. Because of the abnormal morphology of *mpk3 mpk6 GVG:MPK6* seedlings, multiple leaves were used for the ROS-burst assay (Figure S10a), while single leaves were used in all other ROS-burst analyses (Figure S10b). After

overnight incubation, 1 mL of assay solution with 5 μM luminol and 10 μg/mL horseradish peroxidase plus 60 nM flg22 (final concentration 30 nM) was added to each well using a repeat pipette and luminescence was recorded immediately using a photon-counting camera (Photek, http://www.photek.com). NA-PP1-pretreatment of *MPK6SR* leaf samples was done by adding NA-PP1 stock solution into the bathing water at the indicated time prior to the addition of assay mixture. Equal volume of DMSO solvent was used in the control.

Protein extraction, immunoblot analysis, and in-gel kinase activity assay

Protein was extracted from seedlings and stored at -80°C as previously described (Liu and Zhang 2004). The concentration of protein extracts was determined using the Bio-Rad protein assay kit (Bio-Rad, CA) with BSA as the standard. Immunoblot detection of MAPKs and tagged transgene products was performed as previously described (Liu and Zhang 2004). Anti-MPK3, anti-MPK6, and anti-MPK4 antibodies were purchased from Sigma (http://www.sigmaaldrich.com). MAPK activation was detected by either in-gel kinase activity assay using myelin basic protein (MBP) as the substrate (Yang *et al.*, 2001, Zhang and Klessig 1997) or immunoblot analysis using anti-pTEpY (anti-phospho-p44/42-ERK; CST, http://www.cellsignal.com/) as described (Tsuda *et al.*, 2009).

RNA extraction and quantitative RT-PCR analysis

Total RNA was extracted using Trizol reagent (Invitrogen) according to the manufacturer's instructions. After an additional ethanol precipitation and DNase treatment, 1 μg of total RNA were used for reverse transcription (RT). Quantitative PCR analysis was performed using an Optican™ 2 real-time PCR machine (MJ Research). After normalization to an *EF1α* control, the relative levels of gene expression were calculated. The primers used for qRT-PCR were *EF1α* (At5g60390, 5′TGAGCACGCTCTTCTTGCTTTCA3′ and 5′GGTGGTGGCATCCATCTTGTTACA3′), and *AtRbohD* (At5g47910: 5′ATGTACGCTCAGGTAATCGTCTC3′ and 5′GTGGCTGAGATTATTAGTCTTAGTGCT3′).

Supplementary Material

Refer to Web version on PubMed Central for supplementary material.

Acknowledgments

This research was supported by the third stage of Zhejiang University 985 Project #118000-193411801 and a fellowship from the Chinese Scholarship Council to Juan Xu, NSFC grants 30870220 and 30721062 to Dongtao Ren, NSF grants MCB-0543109 and IOS-0743957 to Shuqun Zhang, and NIH grant R21GM088517 and NSF Career Award DBI-0953839 to Xiaoqin Zou.

References

Alonso JM, Stepanova AN, Leisse TJ, Kim CJ, Chen H, Shinn P, Stevenson DK, Zimmerman J, Barajas P, Cheuk R, Gadrinab C, Heller C, Jeske A, Koesema E, Meyers CC, Parker H, Prednis L, Ansari Y, Choy N, Deen H, Geralt M, Hazari N, Hom E, Karnes M, Mulholland C, Ndubaku R, Schmidt I, Guzman P, Aguilar-Henonin L, Schmid M, Weigel D, Carter DE, Marchand T, Risseeuw E, Brogden D, Zeko A, Crosby WL, Berry CC, Ecker JR. Genome-wide insertional mutagenesis of *Arabidopsis thaliana*. Science. 2003; 301:653–657. [PubMed: 12893945]

Apel K, Hirt H. Reactive oxygen species: metabolism, oxidative stress, and signal transduction. Annu Rev Plant Biol. 2004; 55:373–399. [PubMed: 15377225]

Asai S, Ohta K, Yoshioka H. MAPK signaling regulates nitric oxide and NADPH oxidase-dependent oxidative bursts in *Nicotiana benthamiana*. Plant Cell. 2008; 20:1390–1406. [PubMed: 18515503]

Asai T, Tena G, Plotnikova J, Willmann MR, Chiu WL, Gomez-Gomez L, Boller T, Ausubel FM, Sheen J. MAP kinase signalling cascade in Arabidopsis innate immunity. Nature. 2002; 415:977–983. [PubMed: 11875555]

Ausubel FM. Are innate immune signaling pathways in plants and animals conserved? Nat Immunol. 2005; 6:973–979. [PubMed: 16177805]

Bethke G, Pecher P, Eschen-Lippold L, Tsuda K, Katagiri F, Glazebrook J, Scheel D, Lee J. Activation of the Arabidopsis thaliana mitogen-activated protein kinase MPK11 by the flagellin-derived elicitor peptide, flg22. Mol Plant-Microbe Interact. 2012; 25:471–480. [PubMed: 22204645]

Bishop AC, Ubersax JA, Petsch DT, Matheos DP, Gray NS, Blethrow J, Shimizu E, Tsien JZ, Schultz PG, Rose MD, Wood JL, Morgan DO, Shokat KM. A chemical switch for inhibitor-sensitive alleles of any protein kinase. Nature. 2000; 407:395–401. [PubMed: 11014197]

Boller T, Felix G. A renaissance of elicitors: perception of microbe-associated molecular patterns and danger signals by pattern-recognition receptors. Annu Rev Plant Biol. 2009; 60:379–406. [PubMed: 19400727]

Chisholm ST, Coaker G, Day B, Staskawicz BJ. Host-microbe interactions: shaping the evolution of the plant immune response. Cell. 2006; 124:803–814. [PubMed: 16497589]

Cho SK, Larue CT, Chevalier D, Wang H, Jinn TL, Zhang S, Walker JC. Regulation of floral organ abscission in *Arabidopsis thaliana*. Proc Natl Acad Sci USA. 2008; 105:15629–15634. [PubMed: 18809915]

Dangl JL, Jones JDG. Plant pathogens and integrated defense responses to infection. Nature. 2001; 411:826–833. [PubMed: 11459065]

del Pozo O, Pedley KF, Martin GB. MAPKKKa is a positive regulator of cell death associated with both plant immunity and disease. EMBO J. 2004; 23:3072–3082. [PubMed: 15272302]

Dixon RA. Natural products and plant disease resistance. Nature. 2001; 411:843–847. [PubMed: 11459067]

Durrant WE, Dong X. Systemic acquired resistance. Annu Rev Phytopathol. 2004; 42:185–209. [PubMed: 15283665]

Galletti R, Ferrari S, De Lorenzo G. Arabidopsis MPK3 and MPK6 play different roles in basal and oligogalacturonide-or flagellin-induced resistance against *Botrytis cinerea*. Plant physiol. 2011; 157:804–814. [PubMed: 21803860]

Glazebrook J. Contrasting mechanisms of defense against biotrphic and necrotrophic pathogens. Annu Rev Phytopathol. 2005; 43:205–227. [PubMed: 16078883]

Gómez-Gómez L, Boller T. FLS2: A LRR receptor-like kinase involved in recognition of the flagellin elicitor in *Arabidopsis*. Mol Cell. 2000; 5:1–20. [PubMed: 10678164]

Gómez-Gómez L, Felix G, Boller T. A single locus determines sensitivity to bacterial flagellin in *Arabidopsis thaliana*. Plant J. 1999; 18:277–284. [PubMed: 10377993]

Greenberg JT, Yao N. The role and regulation of programmed cell death in plant-pathogen interactions. Cell Microbiol. 2004; 6:201–211. [PubMed: 14764104]

Han L, Li GJ, Yang KY, Mao G, Wang R, Liu Y, Zhang S. Mitogen-activated protein kinase 3 and 6 regulate *Botrytis cinerea*-induced ethylene production in *Arabidopsis*. Plant J. 2010; 64:114–127. [PubMed: 20659280]

Ichimura K, Casais C, Peck SC, Shinozaki K, Shirasu K. MEKK1 is required for MPK4 activation and regulates tissue-specific and temperature-dependent cell death in Arabidopsis. J Biol Chem. 2006; 281:36969–36976. [PubMed: 17023433]

Ichimura K, Shinozaki K, Tena G, Sheen J, Henry Y, Champion A, Kreis M, Zhang S, Hirt H, Wilson C, Heberle-Bors E, Ellis BE, Morris PC, Innes RW, Ecker JR, Scheel D, Klessig DF, Machida Y, Mundy J, Ohashi Y, Walker JC. Mitogen-activated protein kinase cascades in plants: a new nomenclature. Trends Plant Sci. 2002; 7:301–308. [PubMed: 12119167]

Jones JDG, Dangl JL. The plant immune system. Nature. 2006; 444:323. [PubMed: 17108957]

Kinoshita T, Warizaya M, Ohori M, Sato K, Neya M, Fujii T. Crystal structure of human ERK2 complexed with a pyrazolo[3,4-c]pyridazine derivative. Bioorg Med Chem Lett. 2006; 16:55–58. [PubMed: 16242327]

Knowles PP, Murray-Rust J, Kjær S, Scott RP, Hanrahan S, Santoro M, Ibanez CF, McDonald NQ. Structure and chemical inhibition of the RET tyrosine kinase domain. J Biol Chem. 2006; 281:33577–33587. [PubMed: 16928683]

Kovtun Y, Chiu WL, Tena G, Sheen J. Functional analysis of oxidative stress-activated mitogen-activated protein kinase cascade in plants. Proc Natl Acad Sci USA. 2000; 97:2940–2945. [PubMed: 10717008]

Kroj T, Rudd JJ, Nürnberger T, Gäbler Y, Lee J, Scheel D. Mitogen-activated protein kinases play an essential role in oxidative burst-independent expression of pathogenesis-related genes in parsley. J Biol Chem. 2003; 278:2256–2264. [PubMed: 12426314]

Lamb C, Dixon RA. The oxidative burst in plant disease resistance. Annu Rev Plant Biol. 1997; 48:251–275.

Ligterink W, Kroj T, zur Nieden U, Hirt H, Scheel D. Receptor-mediated activation of a MAP kinase in pathogen defense of plants. Science. 1997; 276:2054–2057. [PubMed: 9197271]

Liu Y, Ren D, Pike S, Pallardy S, Gassmann W, Zhang S. Chloroplast-generated reactive oxygen species are involved in hypersensitive response-like cell death mediated by a mitogen-activated protein kinase cascade. Plant J. 2007; 51:941–954. [PubMed: 17651371]

Liu Y, Zhang S. Phosphorylation of 1-aminocyclopropane-1-carboxylic acid synthase by MPK6, a stress-responsive mitogen-activated protein kinase, induces ethylene biosynthesis in *Arabidopsis*. Plant Cell. 2004; 16:3386–3399. [PubMed: 15539472]

Lukowitz W, Roeder A, Parmenter D, Somerville C. A MAPKK kinase gene regulates extra-embryonic cell fate in *Arabidopsis*. Cell. 2004; 116:109–119. [PubMed: 14718171]

Mao G, Meng X, Liu Y, Zheng Z, Chen Z, Zhang S. Phosphorylation of a WRKY transcription factor by two pathogen-responsive MAPKs drives phytoalexin biosynthesis in *Arabidopsis*. Plant Cell. 2011; 23:1639–1653. [PubMed: 21498677]

Marti-Renom MA, Stuart AC, Fiser A, Sanchez R, Melo F, Sali A. Comparative protein structure modeling of genes and genomes. Annu Rev Biophys Biomol Struct. 2000; 29:291–325. [PubMed: 10940251]

Martin GB, Bogdanove AJ, Sessa G. Understanding the functions of plant disease resistance proteins. Annu Rev Plant Biol. 2003; 54:23–61. [PubMed: 14502984]

Meng X, Wang H, He Y, Liu Y, Walker JC, Torii KU, Zhang S. A MAPK cascade downstream of ERECTA receptor-like protein kinase regulates Arabidopsis inflorescence architecture by promoting localized cell proliferation. Plant Cell. 2012; 24:4948–4960. [PubMed: 23263767]

Meng X, Zhang S. MAPK cascade in disease resistance signaling. Annu Rev Phytopathol. 2013; 51:245–266. [PubMed: 23663002]

Mersmann S, Bourdais G, Rietz S, Robatzek S. Ethylene signaling regulates accumulation of the FLS2 receptor and is required for the oxidative burst contributing to plant immunity. Plant physiol. 2010; 154:391–400. [PubMed: 20592040]

Miya A, Albert P, Shinya T, Desaki Y, Ichimura K, Shirasu K, Narusaka Y, Kawakami N, Kaku H, Shibuya N. CERK1, a LysM receptor kinase, is essential for chitin elicitor signaling in *Arabidopsis*. Proc Natl Acad Sci USA. 2007; 104:19613–19618. [PubMed: 18042724]

Nakagami H, Soukupová H, Schikora A, Zárský V, Hirt H. A mitogen-activated protein kinase kinase kinase mediates reactive oxygen species homeostasis in *Arabidopsis*. J Biol Chem. 2006; 281:38697–38704. [PubMed: 17043356]

Petersen M, Brodersen P, Naested H, Andreasson E, Lindhart U, Johansen B, Nielsen HB, Lacy M, Austin MJ, Parker JE, Sharma SB, Klessig DF, Martienssen R, Mattsson O, Jensen AB, Mundy J. Arabidopsis MAP kinase 4 negatively regulates systemic acquired resistance. Cell. 2000; 103:1111–1120. [PubMed: 11163186]

Pettersen EF, Goddard TD, Huang CC, Couch GS, Greenblatt DM, Meng EC, Ferrin TE. UCSF Chimera—A visualization system for exploratory research and analysis. J Comput Chem. 2004; 25:1605–1612. [PubMed: 15264254]

Pitzschke A, Hirt H. Disentangling the complexity of mitogen-activated protein kinases and reactive oxygen species signaling. Plant Physiology. 2009; 149:606–615. [PubMed: 19201916]

Qiu JL, Zhou L, Yun BW, Nielsen HB, Fiil BK, Petersen K, MacKinlay J, Loake GJ, Mundy J, Morris PC. Arabidopsis mitogen-activated protein kinase kinases MKK1 and MKK2 have overlapping functions in defense signaling mediated by MEKK1, MPK4, and MKS1. Plant Physiol. 2008; 148:212–222. [PubMed: 18599650]

Ranf S, Eschen-Lippold L, Pecher P, Lee J, Scheel D. Interplay between calcium signalling and early signalling elements during defence responses to microbe-or damage-associated molecular patterns. Plant J. 2011; 68:100–113. [PubMed: 21668535]

Ren D, Liu Y, Yang KY, Han L, Mao G, Glazebrook J, Zhang S. A fungal-responsive MAPK cascade regulates phytoalexin biosynthesis in *Arabidopsis*. Proc Natl Acad Sci USA. 2008; 105:5638–5643. [PubMed: 18378893]

Ren D, Yang H, Zhang S. Cell death mediated by mitogen-activated protein kinase pathway is associated with the generation of hydrogen peroxide in *Arabidopsis*. J Biol Chem. 2002; 277:559–565. [PubMed: 11687590]

Rodriguez MCS, Petersen M, Mundy J. Mitogen-activated protein kinase signaling in plants. Annu Rev Plant Biol. 2010; 61:621–649. [PubMed: 20441529]

Romeis T, Piedras P, Zhang S, Klessig DF, Hirt H, Jones J. Rapid Avr9-and Cf-9-dependent activation of MAP kinases in tobacco cell cultures and leaves: convergence of resistance gene, elicitor, wound and salicylate responses. Plant Cell. 1999; 11:273–287. [PubMed: 9927644]

Schweighofer A, Kazanaviciute V, Scheikl E, Teige M, Doczi R, Hirt H, Schwanninger M, Kant M, Schuurink R, Mauch F. The PP2C-type phosphatase AP2C1, which negatively regulates MPK4 and MPK6, modulates innate immunity, jasmonic acid, and ethylene levels in *Arabidopsis*. Plant Cell. 2007; 19:2213–2224. [PubMed: 17630279]

Segonzac C, Feike D, Gimenez-Ibanez S, Hann DR, Zipfel C, Rathjen JP. Hierarchy and roles of pathogen-associated molecular pattern-induced responses in *Nicotiana benthamiana*. Plant physiol. 2011; 156:687–699. [PubMed: 21478366]

Shirasu K, Nakajima H, Rajasekhar VK, Dixon RA, Lamb C. Salicylic acid potentiates an agonist-dependent gain control that amplifies pathogen signals in the activation of defense mechanisms. Plant Cell. 1997; 9:261–270. [PubMed: 9061956]

Shpak ED, Berthiaume CT, Hill EJ, Torii KU. Synergistic interaction of three ERECTA-family receptor-like kinases controls Arabidopsis organ growth and flower development by promoting cell proliferation. Development. 2004; 131:1491–1501. [PubMed: 14985254]

Suarez-Rodriguez MC, Adams-Phillips L, Liu Y, Wang H, Su SH, Jester PJ, Zhang S, Bent AF, Krysan PJ. MEKK1 is required for flg22-induced MPK4 activation in Arabidopsis plants. Plant Physiol. 2007; 143:661–669. [PubMed: 17142480]

Thordal-Christensen H, Zhang Z, Wei Y, Collinge DB. Subcellular localization of H_2O_2 in plants. H_2O_2 accumulation in papillae and hypersensitive response during the barley--powdery mildew interaction. Plant J. 1997; 11:1187–1194.

Tocquin P, Corbesier L, Havelange A, Pieltain A, Kurtem E, Bernier G, Périlleux C. A novel high efficiency, low maintenance, hydroponic system for synchronous growth and flowering of *Arabidopsis thaliana*. BMC Plant Biol. 2003; 3:2. [PubMed: 12556248]

Torres MA, Dangl JL. Functions of the respiratory burst oxidase in biotic interactions, abiotic stress and development. Curr Opin Plant Biol. 2005; 8:397–403. [PubMed: 15939662]

Torres MA, Dangl JL, Jones JDG. Arabidopsis $gp91^{phox}$ homolog *AtrbohD* and *AtrbohF* are required for accumulation of reactive oxygen intermediates in the plant defense response. Proc Natl Acad Sci USA. 2002; 99:523–528. [PubMed: 11756669]

Tsuda K, Sato M, Stoddard T, Glazebrook J, Katagiri F. Network properties of robust immunity in plants. PLoS Genet. 2009; 5:e1000772. [PubMed: 20011122]

Wan J, Zhang XC, Neece D, Ramonell KM, Clough S, Kim Sy, Stacey MG, Stacey G. A LysM receptor-like kinase plays a critical role in chitin signaling and fungal resistance in *Arabidopsis*. Plant Cell. 2008; 20:471–481. [PubMed: 18263776]

Wang H, Liu Y, Bruffett K, Lee J, Hause G, Walker JC, Zhang S. Haplo-insufficiency of MPK3 in MPK6 mutant background uncovers a novel function of these two MAPKs in Arabidopsis ovule development. Plant Cell. 2008; 20:602–613. [PubMed: 18364464]

Wang H, Ngwenyama N, Liu Y, Walker JC, Zhang S. Stomatal development and patterning are regulated by environmentally responsive MAP kinases in *Arabidopsis*. Plant Cell. 2007; 19:63–73. [PubMed: 17259259]

Yang KY, Liu Y, Zhang S. Activation of a mitogen-activated protein kinase pathway is involved in disease resistance in tobacco. Proc Natl Acad Sci USA. 2001; 98:741–746. [PubMed: 11209069]

Yoshioka H, Numata N, Nakajima K, Katou S, Kawakita K, Rowland O, Jones JDG, Doke N. *Nicotiana benthamiana* gp91phox homologs *NbrbohA* and *NbrbohB* participate in H_2O_2 accumulation and resistance to *Phytophthora infestans*. Plant Cell. 2003; 15:706–718. [PubMed: 12615943]

Yuasa T, Ichimura K, Mizoguchi T, Shinozaki K. Oxidative stress activates AtMPK6, an Arabidopsis homologue of MAP kinase. Plant Cell Physiol. 2001; 42:1012–1016. [PubMed: 11577197]

Zhang J, Shao F, Li Y, Cui H, Chen L, Li H, Zou Y, Long C, Lan L, Chai J, Chen S, Tang X, Zhou JM. A *Pseudomonas syringae* effector inactivates MAPKs to suppress PAMP-induced immunity in plants. Cell Host Microbe. 2007; 1:175–185. [PubMed: 18005697]

Zhang S, Klessig DF. Salicylic acid activates a 48 kD MAP kinase in tobacco. Plant Cell. 1997; 9:809–824. [PubMed: 9165755]

Zipfel C, Kunze G, Chinchilla D, Caniard A, Jones JDG, Boller T, Felix G. Perception of the bacterial PAMP EF-Tu by the receptor EFR restricts *Agrobacterium*-mediated transformation. Cell. 2006; 125:749–760. [PubMed: 16713565]

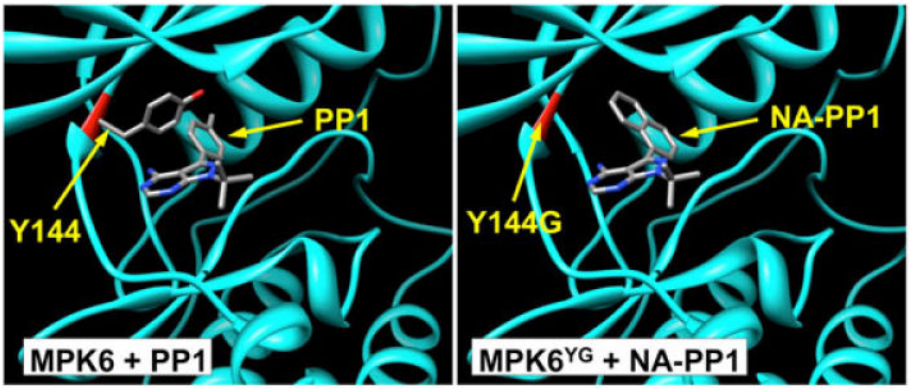

Figure 1.

Activation of Arabidopsis MPK3/MPK6 induces ROS generation in chloroplast, but not Rboh NADPH oxidase-mediated ROS burst.

(**a**) ROS generation in the chloroplasts of the conditional gain-of-function *DD* seedlings after DEX treatment. Two-week-old *GVG:NtMEK2*^{DD} (*DD*) and control *GVG:NtMEK2*^{KR} (*KR*) transgenic Arabidopsis seedlings were treated with 1 μM DEX. *In situ* ROS generation was detected by DAB staining after 9 hr DEX treatment. Bar = 15 μm.

(**b**) Luminol-based ROS assay failed to detect the Rboh NADPH oxidase-mediated ROS burst in *DD* seedlings treated with DEX. ROS production was detected by luminol-based assay at various times after DEX treatment. Data shown were from seedlings after 3 hr DEX treatment. Error bars indicate SD (n = 3).

(**c**) Activation of MPK3/MPK6 in *DD*, but not *KR*, seedlings after DEX treatment. MAPK activity was determined by the in-gel kinase assay with myelin basic protein as a substrate.

(**d**) Activation of MPK3/MPK6 in *DD* plants partially compromises the flg22-induced ROS burst. After 3 hr DEX treatment, ROS burst was monitored by luminol-based assay immediately after the addition of flg22 (30 nM). Error bars indicate SD (n = 3). Different letters indicate statistically significant different groups ($p<0.05$).

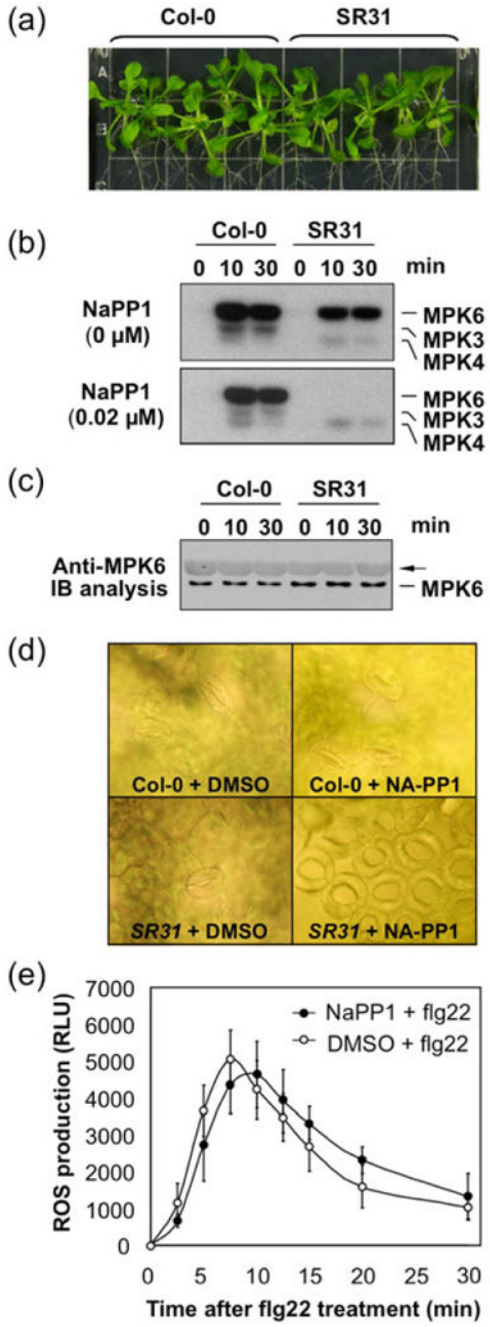

Figure 2.

MPK3 and MPK6 are not essential to the ROS burst induced by flg22.

(**a**) *MPK3* and *MPK6* single mutant seedlings showed normal ROS burst after flg22 treatment. Two-week-old wild-type control (Col-0), *mpk3*, and *mpk6* single mutant seedlings were treated with flg22 (30 nM). ROS burst was monitored by luminol-based assay. Error bars indicate SD (n = 3).

(**b**) ROS burst in the conditionally rescued *mpk3 mpk6* double mutant seedlings was mostly intact. Two-week-old wild-type control (Col-0), and rescued *mpk3 mpk6* double mutant

seedlings were treated with flg22 (30 nM). ROS burst was monitored by luminol-based assay. Error bars indicate SD (n = 3). Single and double asterisks above the data points indicate differences that are statistically significant ($p<0.05$) and statistically very significant ($p<0.01$), respectively.

(**c**) Activation and levels of MAPKs in Col-0, *mpk3*, *mpk6*, and rescued *mpk3 mpk6* seedlings treated with flg22. MAPK activation was detected by in-gel kinase assay using MBP as a substrate. The levels of MPK6 and MPK4 (middle) or MPK3 (bottom) were detected by immunoblot analysis using a mixture of anti-MPK6 and anti-MPK4 antibodies (middle) or anti-MPK3 antibody (bottom). Asterisk indicates the non-specific binding of Rubisco large subunit by the secondary antibody.

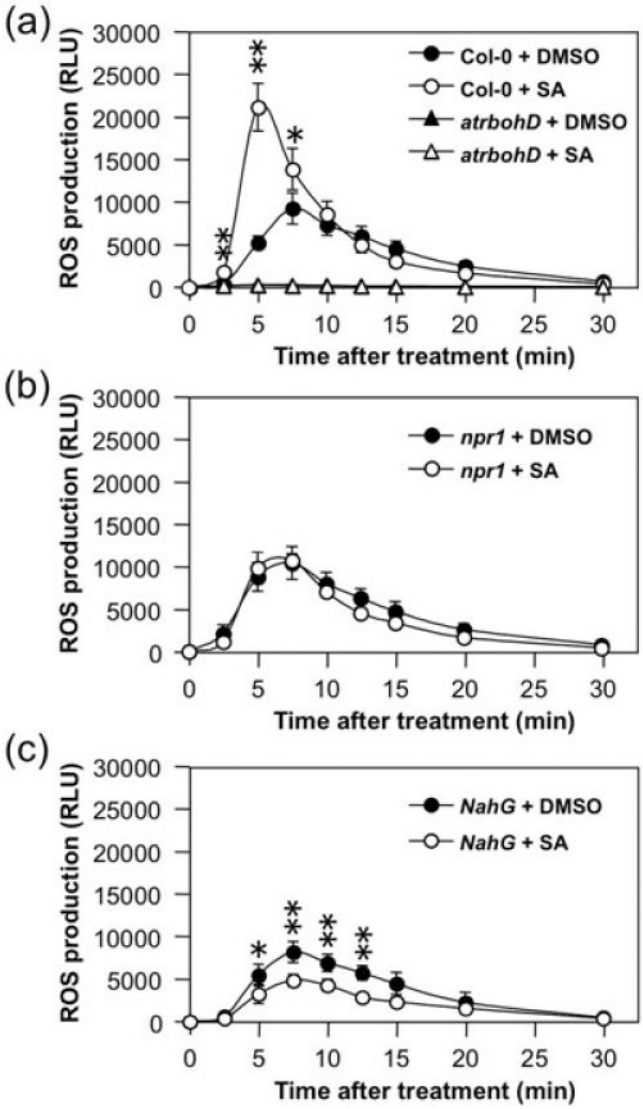

Figure 3.

Binding of PP1 to wild-type MPK6, and NA-PP1 to the sensitized MPK6 variants, $MPK6^{YG}$.

NA-PP1, an analog of PP1 with bulky side chain, would have atomic clashes with the Tyr residue in the ATP binding pocket of wild-type MPK6, but not so with the sensitized $MPK6^{YG}$ variants (right panel). In contrast, PP1 can access the ATP-binding pocket of wild-type kinases (left panels). The three-dimensional atomic structure of MPK6 was built based on the crystal structure of human ERK2 (PDB entry: 1WZY) using the MODELLER software. The three dimensional atomic structure of NA-PP1 was built using Chimera based on the crystal structure of PP1 (PDB entry: 2IVV). The binding mode of MPK6 with PP1, or the sensitized MPK6 ($MPK6^{YG}$) with NA-PP1 was produced by superimposing MPK6 or $MPK6^{YG}$ with the crystal structure of RET tyrosine kinase bound with PP1 using Chimera software. In both panels, the protein is plotted in ribbon diagram. The backbones of Y144 in wild-type MPK6 and backbones of G144 in $MPK6^{YG}$ are highlighted in red. The ligand and

Y144 in MPK6 are displayed in stick mode and colored by atom types. Red: oxygens; blue: nitrogens, and grey: carbons. Hydrogen atoms are not shown.

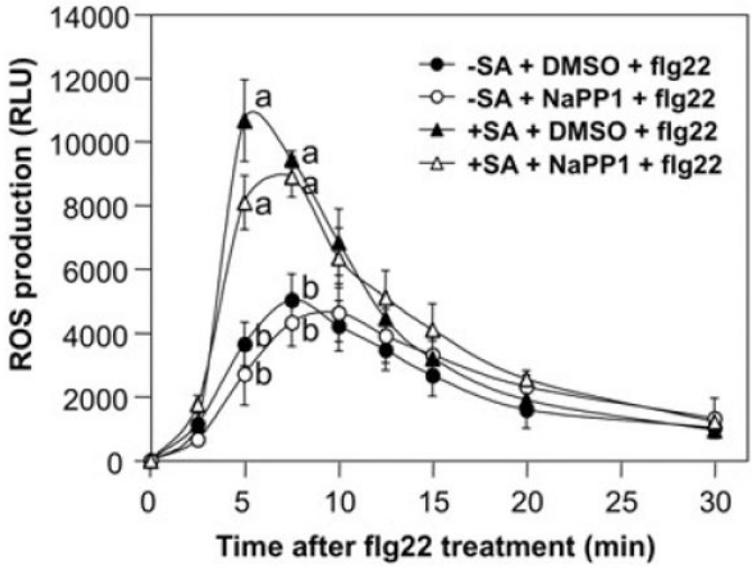

Figure 4.

Normal flg22-induced ROS burst in the *mpk3 mpk6* double mutant system generated using a chemical genetic approach.

(**a**) Complete rescue of the developmental defects of *mpk3 mpk6* by a native promoter-driven inhibitor-sensitized variant of MPK6 (P_{MAPK6}:$MPK6^{YG}$). *SR31*, sensitized MPK6 variant rescued line #31 (genotype: *mpk3 mpk6* P_{MAPK6}:$MPK6^{YG}$). Image of 2-week-old seedlings was taken.

(**b**) *In vitro* inhibition of $MPK6^{YG}$ by low concentration of NA-PP1 inhibitor. Two-week-old Col-0 and *SR31* seedlings were treated with flg22 for 10 and 30 min. Total proteins were extracted and 10 μg of each was analyzed by in-gel kinase assay in the absence (0 μM) and presence of 0.02 μM NA-PP1 in the reaction solution.

(**c**) Levels of MPK6 protein in Col-0 and $MPK6^{YG}$ in *SR31* seedlings were determined by immunoblot analysis using anti-MPK6 antibody. Arrow indicates Rubisco protein weakly bound by the secondary antibody.

(**d**) *In vivo* inhibition of $MPK6^{YG}$ as indicated by the development of clustered stomata in the presence of NA-PP1 inhibitor. In the presence of 0.5 μM NA-PP1, Col-0 seedlings showed normal stomata morphology, while *SR31* seedlings showed clustered stomata, demonstrating the effectiveness of NA-PP1 in inhibiting $MPK6^{YG}$ activity *in vivo*. Seeds were germinated on plain MS plates and five-days old seedlings were transferred to MS plates with 0.5 μM NA-PP1 inhibitor or equal volume of DMSO solvent control. Seven days later, true leaves were sampled for microscopic observation and imaging.

(**e**) Similar ROS burst in *SR31* seedlings in the presence and absence of NA-PP1 inhibitor. Two-week-old SR31 seedlings were pre-treated with either NA-PP1 (1 μM) or equal volume of DMSO for 30 min, and then treated with flg22 (30nM). Error bars indicate SD (n = 3).

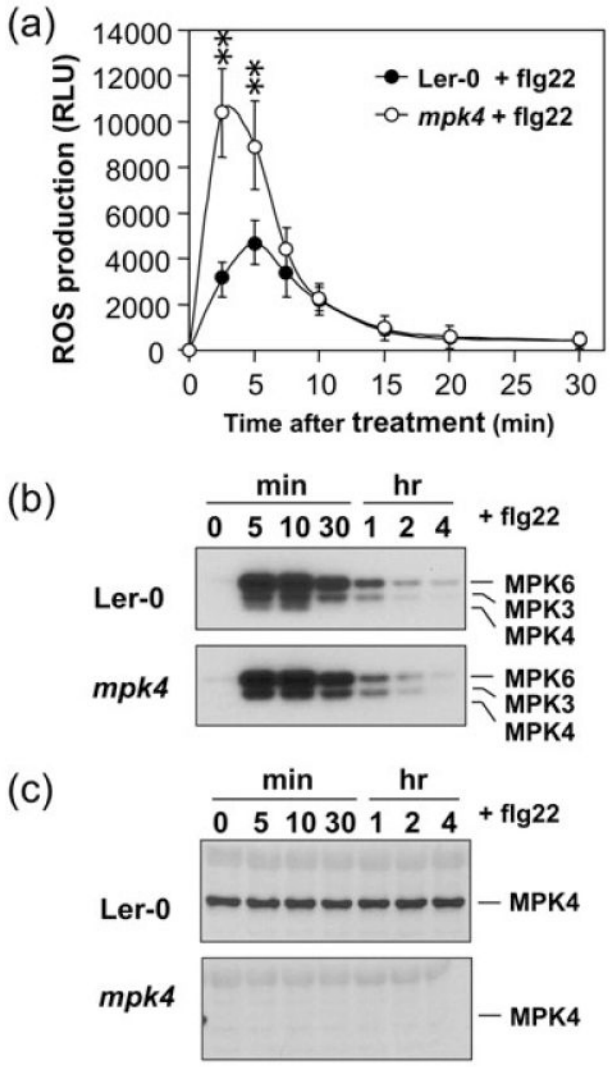

Figure 5.

Salicylic acid (SA) potentiates flg22-induced ROS burst.

Two-week-old Col-0, *atrbohD*, *npr1*, and *NahG* seedlings were pre-treated with SA (100 μM) or equal volume of DMSO solvent for two days, and then treated with flg22 (30 nM). ROS burst was monitored by luminol-based ROS detection using a photon-counting camera. Error bars indicate SD (n = 3). Single and double asterisks above the data points indicate differences that are statistically significant ($p<0.05$) and statistically very significant ($p<0.01$), respectively.

(**a**) Enhance ROS burst by SA pre-treatment is dependent on functional *AtRbohD* gene.

(**b**) SA-potentiation of ROS burst is dependent on *NPR1*.

(**c**) Enhanced ROS burst in seedlings with SA pretreatment is abolished in *NahG* background.

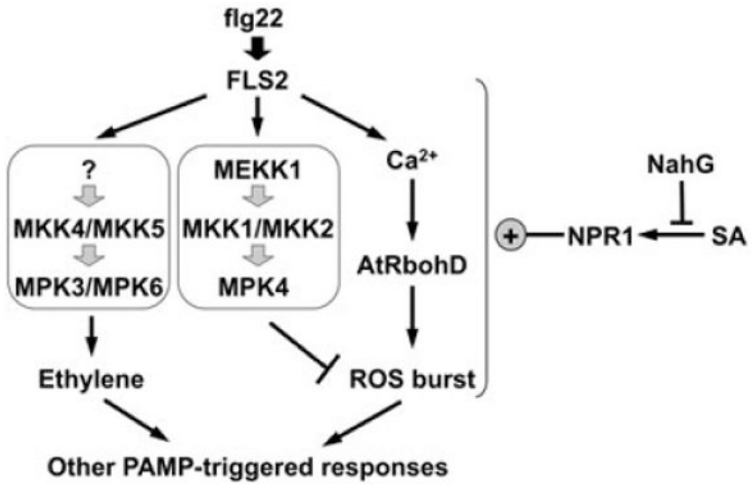

Figure 6.

MPK3 and MPK6 are not required for the enhanced ROS burst after SA pretreatment. Two-week-old *SR31* seedlings were pre-treated with SA (100 μM) or equal volume of DMSO solvent for two days. Before flg22 treatment, the seedlings were pre-treated with either NA-PP1 (1 μM) or equal volume of DMSO for 30 min, and then flg22 (30 nM) was then added. ROS burst was monitored by luminol-based ROS detection using a photon-counting camera. Error bars indicate SD (n = 3). Different letters indicate statistically significant different groups ($p<0.05$).

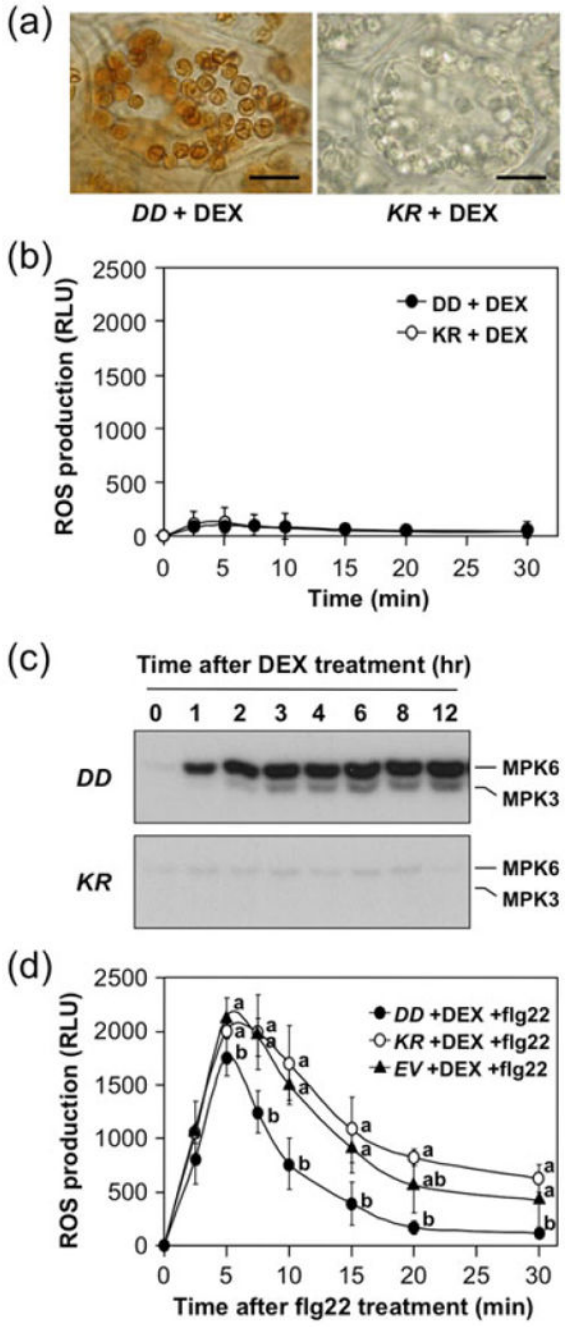

Figure 7.

Mutation of *MPK4* enhances ROS burst induced by flg22 in Arabidopsis.

(**a**) The flg22-induced ROS burst is enhanced in *mpk4* mutant. Two-week-old wild-type (Ler-0) and *mpk4* seedlings were treated with flg22 (30 nM). ROS burst was monitored by luminol-based ROS detection using a photon-counting camera. Error bars indicate SD (n = 3). Double asterisks above the data points indicate differences that are statistically very significant ($p<0.01$).

(**b**) Absence of MPK4 activity in the *mpk4* seedlings after flg22 treatment. MAPK activation was detected by in-gel kinase assay using MBP as a substrate.
(**c**) Absence of MPK4 protein in the *mpk4* seedlings used for experiment. The levels of MPK4 protein in samples prepared in (b) were detected by immunoblot analysis using an anti-MPK4 antibody.

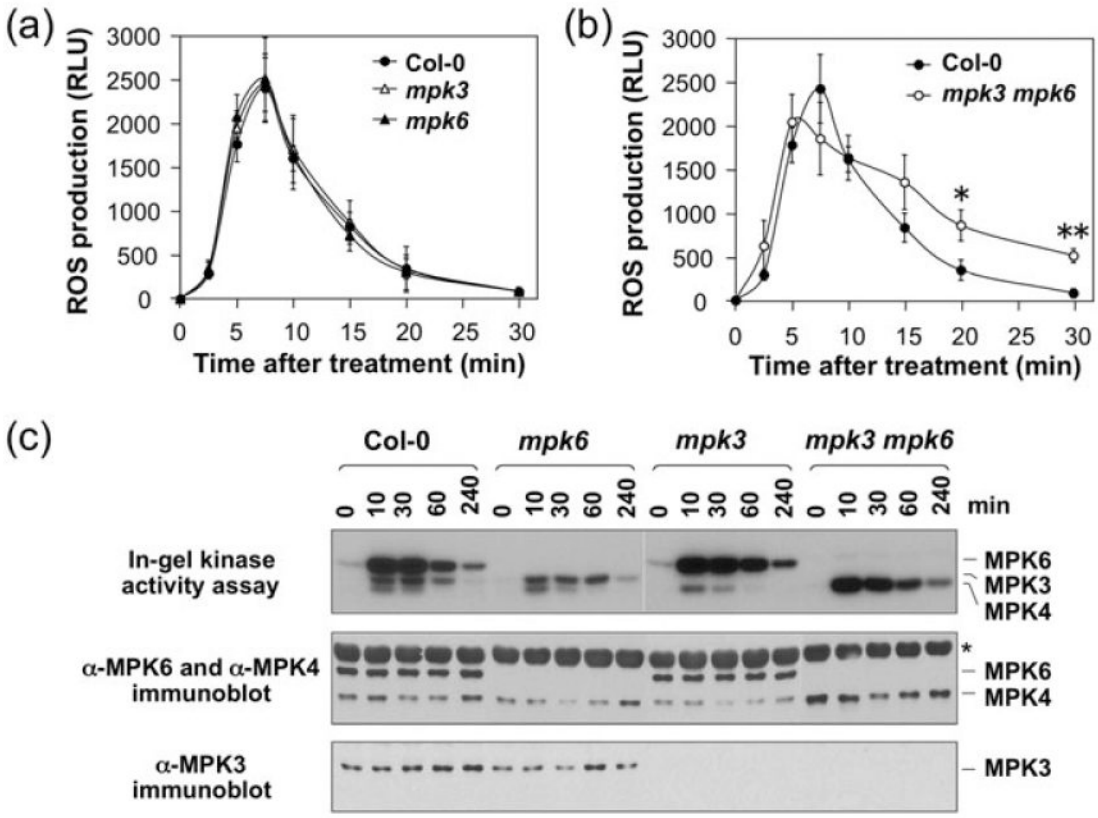

Figure 8.

ROS burst and MAPK activation are two independent signaling events after plant sensing of flg22.

FLS2-mediated sensing of flg22 activated two MAPK cascades. Among them, MPK3/MPK6 cascade is independent of *AtRbohD*-mediated ROS burst. In contrast, the lack of functional *MPK4* results in an enhanced ROS burst, similar to the potentiation effect seen in SA-pretreated seedlings. SA-enhanced ROS burst is dependent on *NPR1* and can be abolished by *NahG* transgene.